

https://doi.org/10.1070/QEL16656

Trapping of thulium atoms in a cavity-enhanced optical lattice near a magic wavelength of 814.5 nm

E.S. Kalganova, A.A. Golovizin, D.O. Shevnin, D.O. Tregubov, K.Yu. Khabarova, V.N. Sorokin, N.N. Kolachevsky

Abstract. **A cavity-enhanced optical lattice at a wavelength of 814.5 nm for thulium atoms is designed and its characteristics are investigated. The parametric resonances at the vibrational frequencies of the trap are measured. The enhancement cavity will be applied to search for the magic wavelength of the clock transition at 1.14 μm in thulium atoms.**

Keywords: *frequency standard, optical lattice, enhancement cavity, parametric resonances, ultracold atoms, thulium.*

1. Introduction

The precision of modern optical clocks based on ensembles of neutral atoms in optical lattices and single ions achieves a few parts in 10^{18} [1, 2], which offers wide possibilities both for fundamental studies [3, 4] and for solving a number of applied problems [5]. In spite of the advances in the development of optical clocks using neutral atoms of strontium [6] and ytterbium [7], as well as some ions (aluminium [8], ytterbium [9]), the search for new prospective atomic systems for frequency standards is still going on [10, 11]. We study the characteristics of the frequency standard based on neutral thulium atoms in an optical lattice. The magnetic dipole transition between the fine-structure components of the ground state at the wavelength 1.14 μm having the natural spectral width 1.4 Hz is chosen as a clock transition in thulium atom. According to the calculations [12], this transition is expected to have a low sensitive to the frequency shift caused by the environmental thermal radiation.

The accuracy of an optical frequency standard is determined mainly by the detailed knowledge of frequency shifts of the clock transition caused by external fields and the capability to control them. For atoms trapped in an optical lattice, one of the most essential frequency shifts of the clock transition is the shift caused by the radiation of the optical lattice itself. To minimise this shift, the optical lattice is to be formed at the so-called magic wavelength, for which the polarisabilities of the upper and lower levels of the clock transition coincide [13]. Commonly, the magic wavelength can be calculated theoretically with an error of a few nanometres [14], whereas its exact value is determined experimentally from the shift of the clock transition frequency depending on the intensity of radiation in the optical lattice [15, 16].

As a rule, in optical frequency standards use is made of optical lattices having a small depth of the order of 10–50 $E_{\rm rec}$, where $E_{\rm rec} = h^2/(2m\lambda^2)$ is the recoil energy; h is the Planck constant; λ is the wavelength of the optical lattice; and m is the atom mass. On the other hand, the use of deeper traps makes it possible to increase the accuracy of determining the magic wavelength position and to study the level shifts, nonlinearly depending on the intensity [17, 18]. The enhancement of the optical lattice using an external cavity allows increasing the range of intensity variation and selecting the specified spatial mode of radiation. Besides an increase in intensity, the use of an enhancement cavity allows a refinement of its value in the trap compared to the case of mere focusing, since the cavity mode size can be determined with high accuracy. The precise determination of intensity, in turn, offers a possibility of reliable measurements of the absolute values of atomic level polarisabilities from the frequency shift in the light field.

In the paper, we present the results of developing an external enhancement cavity for an optical lattice aimed to search for the magic wavelength of the clock transition in thulium atoms in the range 800–860 nm. The efficiency of loading thulium atoms from a magnetooptical trap (MOT) into the optical lattice is measured as a function of the laser radiation power forming the lattice. The spectrum of parametric resonances is studied and the vibrational frequencies of atoms in the optical lattice are measured.

2. Enhancement cavity design

Previously, we have calculated that the preferential magic wavelength for the clock transition in thulium atoms lies in the spectral range 806–815 nm [12]. To create an optical lattice, the radiation of a wavelength-tunable Ti : sapphire laser is used. We use a vertical configuration of the lattice to reduce the probability of tunnelling between the cells [19]. The atoms are loaded into the optical lattice from MOT, described in detail in Refs [20, 21].

Two spherical mirrors, installed outside a vacuum chamber (Fig. 1), formed an external enhancement cavity. The power of radiation in an antinode of the standing wave in the centre of the cavity $P_{\rm c}$ is related to the input power of radiation P_0 by the expression

$$P_{\rm c} = P_0 \frac{T_{\rm in} T_{\rm f}}{(1 - T_{\rm f}^2 \sqrt{R_{\rm in} R_{\rm out}})^2} (1 + T_{\rm f} \sqrt{R_{\rm out}})^2, \qquad (1)$$

E.S. Kalganova, A.A. Golovizin, K.Yu. Khabarova, V.N. Sorokin, N.N. Kolachevsky P.N. Lebedev Physical Institute, Russian Academy of Sciences, Leninsky prosp. 53, 119991 Moscow, Russia; International Centre for Quantum Technologies, ul. Novaya 100, Skolkovo, 143025 Moscow, Russia; e-mail: kalganova.elena@gmail.com;
D.O. Shevnin, D.O. Tregubov P.N. Lebedev Physical Institute, Russian Academy of Sciences, Leninsky prosp. 53, 119991 Moscow, Russia

Received 21 February 2018
Kvantovaya Elektronika **48** (5) 415–418 (2018)
Translated by V.L. Derbov

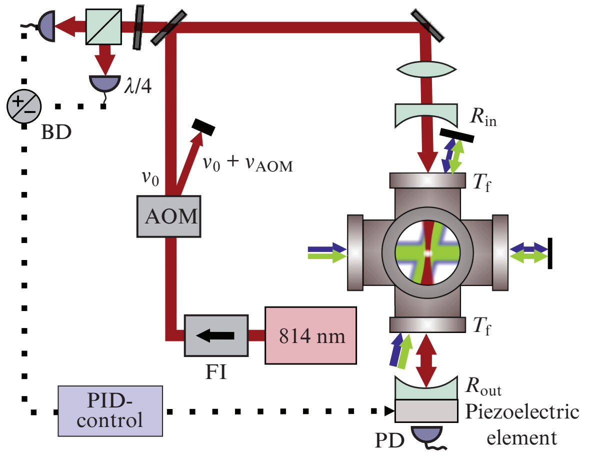

Figure 1. Schematic of the optical lattice enhancement cavity: (FI) Faraday isolator; (PD) photodiode; (BD) balance detector; ν_{AOM} = 39 MHz is the frequency of the acoustooptical modulator (AOM); ν_0 is the radiation optical frequency. The curvature radius of the mirrors is $r_m = 25$ cm, the separation between the mirrors is 481 mm, and the reflection coefficient is $R_{in} = 87\%$ for the input mirror and $R_{out} = 99.99\%$ for the highly reflecting one. Double arrows show the MOT cooling beams.

where T_{in}, R_{in} (T_{out}, R_{out}) are the intensity transmission and reflection coefficients of the input (output) mirror; and T_f is the intensity transmission coefficient of each flange.

The power ehnancement coefficient, defined as a ratio of the powers in the antinodes of the optical lattice in the cavity to that in the absence of the cavity (when the input mirror is absent) is given by

$$K = \frac{T_{in}}{(1 - T_f^2\sqrt{R_{in}R_{out}})^2}. \qquad (2)$$

The total losses measured at the flanges of the vacuum chamber for the wavelengths near 800 nm amount to 13% per roundtrip, i.e., $T_f^4 = 0.87$ for two flanges, each passed forward and backward. To maximise the power of radiation circulating in the cavity and to match the impedances, the reflection coefficient of the entrance mirror should also equal 0.87. The second mirror was chosen to be highly reflecting with the reflection coefficient above 0.99.

The cavity configuration was chosen close to concentric, since it allows essential variation of the waist size by a relatively small change in the separation between the mirrors. For the chosen curvature radius of the mirrors (r_m = 25 cm), the change in the cavity length within 460–495 mm leads to a change in the waist radius w_0 from 133 to 80 μm at the $1/e^2$ intensity level. In the present paper, all measurements were performed in the configuration with the separation between the mirrors equal to 481±1 mm, which corresponds to the waist size of 111.3±1.4 μm. The spatial mode of laser radiation was matched to the cavity mode by performing appropriate measurements and choosing the matching optics.

The cavity transmission peak was locked to the laser frequency using the Hänsch–Couillaud method, and the tuning of the cavity length was implemented by displacing the highly reflecting mirror with a piezoelectric element (Fig. 1) [22]. The feedback bandwidth amounted to 6 kHz. The power of radiation circulating in the cavity was determined using a photodiode installed behind the output mirror of the cavity. The proportionality coefficient U between the radiation power in the cavity and the voltage at the photodiode was measured separately and was used in the subsequent experiments to determine the radiation power in the lattice antinodes. The resulting relative error of the radiation intensity assessment in the trap region ($I = 2P_c/\pi w_0^2 = 2\kappa U/\pi w_0^2$) is determined by the expression

$$\delta I/I = \sqrt{(\delta\kappa/\kappa)^2 + (\delta U/U)^2 + (2\delta w_0/w_0)^2}$$

and equals 6%–10% depending on the power at $\delta k/k = 0.05$, $\delta U = 50$ mV, $U = 0.6$–1.9 V, and $\delta w_0/w_0 = 0.0013$.

The radiation power enhancement coefficient in the cavity is $K = 8.5$, which allows the efficiency of loading atoms from the MOT to the optical lattice to have the values up to 60%. The maximal trap depth in the units of recoil energy is $U_0 = 500E_{rec}$. The dependence of the loading coefficient on the radiation power in the lattice antinodes is presented in Fig. 2. The loading efficiency is limited by the available radiation power, as well as by the spatial overlap of the optical lattice waist with the cloud of atoms in the MOT.

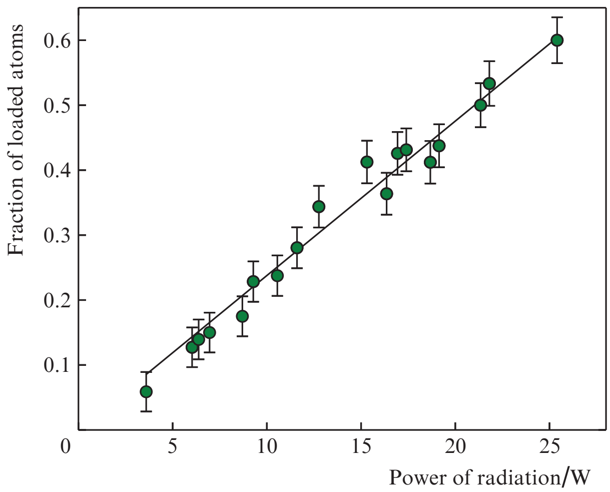

Figure 2. Dependence of the fraction of atoms loaded from the MOT into the optical lattice on the radiation power P_c in the antinodes of the optical lattice (the points show the experimental data, the straight line corresponds to the linear approximation).

3. Parametric resonances

As mentioned above, the enhancement cavity allows one to increase the depth of the trapping potential of the optical lattice and to determine it. One of the ways to determine the depth of the trapping potential is the study of parametric resonances [23]. The potential of a one-dimensional optical lattice, formed by the Gaussian beam overlapping its reflected counterpart and arranged along the z axis is described by the expression

$$U_{lat}(r,z) = -U_0(z)\exp(-2r^2/w_0^2)\cos^2(2\pi z/\lambda), \qquad (3)$$

where $U_0(z) = 4\alpha_g a_0^3 P_c/(cw^2(z))$ is the maximal depth of the lattice; r is the distance from the axis of the optical lattice; α_g is the polarisability of the atom in the ground state; a_0 is the Bohr radius; c is the velocity of light; and $w(z)$ is the Gaussian beam radius at the distance z from the waist along the beam axis. Near the minima, Eqn (3) has the form of a harmonic potential

$$U_{\rm lat}(r,z) = \frac{1}{2}m\omega_r^2 r^2 + \frac{1}{2}m\omega_z^2 z^2, \quad (4)$$

where $\omega_r = 2\pi f_r$ is the transverse vibration frequency; $\omega_z = 2\pi f_z z$ is the longitudinal vibration frequency for the atoms in the lattice;

$$f_r = \frac{2}{\pi w_0^2}\sqrt{\frac{a_0^3\alpha_{\rm g}P_{\rm c}}{cm}}; \quad (5)$$

and

$$f_z = \frac{2}{w_0\lambda}\sqrt{\frac{2a_0^3\alpha_{\rm g}P_{\rm c}}{cm}}. \quad (6)$$

The harmonic modulation of the potential depth, i.e., the power of the radiation forming the lattice at the frequencies $f = 2f_i/n$, where $i = r, z$, and n is an integer, leads to the parametric excitation of atomic transitions between the vibrational energy levels [23], the heating, and the loss of atoms from the trap. Thus, investigating the loss of atoms from the optical lattice as a function of the power modulation frequency, one can determine the longitudinal and transverse eigenfrequencies of the trap.

The experiment on recording the parametric resonances was carried out as follows. The thulium atoms were cooled and trapped in the MOT [20, 21]. In the trapping region, the radiation of the optical lattice was present simultaneously with the MOT. After the cooling cycle, the trapping fields of the MOT were switched off, and part of atoms remained trapped in the optical lattice. The radiation power of the optical lattice was continuously modulated by means of an acousto-optic modulator (AOM) (Fig. 1). The lattice was formed by the zero-order diffracted beam from the AOM, its power being determined by the power of the radio-frequency signal applied to the AOM. The amplitude modulation of the radio-frequency AOM signal led to the modulation of laser radiation power at the same frequency. During the experiment, the enhancement cavity was stabilised. Its transmission bandwidth $\Delta\nu$ amounted to 7 MHz, which essentially exceeded the used modulation frequencies, thanks to which the transmission coefficients for the carrier frequency and for modulation sideband frequencies practically coincided. Thus, the presence of the cavity did not affect the modulation parameters.

We studied two frequency ranges, corresponding to the longitudinal and transverse resonance frequencies of atom vibrations in the optical lattice. The modulation depth was from 2 % to 10 % depending on the resonance strength. In τ = 100 ms after switching off the MOT the number of atoms staying in the optical lattice was measured. The results of the study of the loss of atoms from the lattice are presented in Fig. 3. The experiment was also performed in a different scheme, when, instead of continuous modulation, the lattice intensity was modulated during the first 300 ms after switching the MOT fields off, and then the number of atoms staying in the trap was detected. The results obtained using both methods were similar.

To find the trap vibration frequencies, the contours of parametric resonances near their centres were approximated by quadratic functions. It is seen that in accordance with Eqns (5) and (6) the change of the radiation power in the antinodes of the lattice leads to the shift of the resonance frequency (see insets in Fig. 3). The values of the obtained longitudinal and transverse frequencies are presented in Table 1.

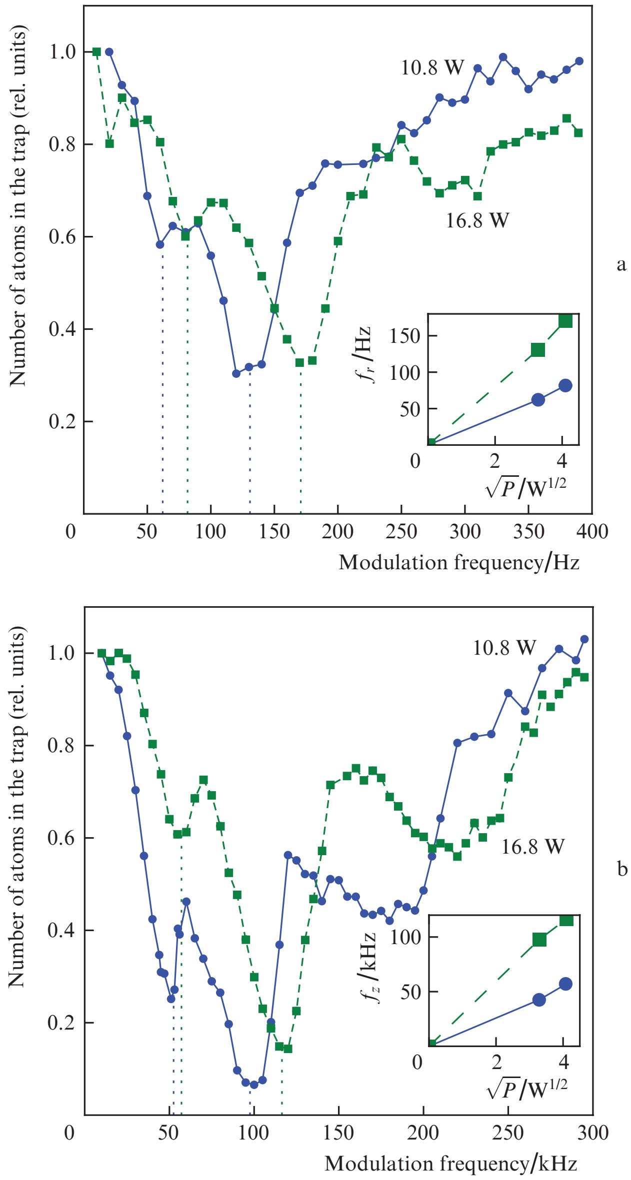

Figure 3. Spectra of (a) low-frequency and (b) high-frequency parametric resonances in the optical lattice. The resonance frequencies are determined using a quadratic approximation of the experimental points near the resonances. In the insets, the shift of the resonance frequency depending on the radiation power in the lattice antinodes is shown.

From the relation of these frequencies [see Eqns (5) and (6)] one can determine the dynamic polarisability of the ground state of the thulium atom at the wavelength 814.5 nm and the size of the optical lattice waist:

$$\alpha_{\rm g} = \frac{f_z^4\lambda^4 cm}{16 f_r^2 a_0^3\pi^2 P_{\rm c}}, \quad (7)$$

$$w_0 = \frac{\lambda}{\sqrt{2}\pi}\frac{f_z}{f_r}. \quad (8)$$

The polarisability calculated using Eqn (7) is $\alpha_{\rm g} = 146\pm44$ a.u. For the calculations we used the vibration frequencies for a deeper potential, corresponding to $P_{\rm c}$ = 16.8 W, where the effect

Table 1. Frequencies of parametric resonances in the studied trap at two values of the radiation power in the loops.

P_c/W	f_r/Hz	$2f_r$/Hz	f_z/kHz	$2f_z$/kHz
10.8	62±10	131±10	52±5	97±7
16.8	82±10	171±10	57±5	116±7

of anharmonicity is smaller. Earlier in Ref. [12] the polarisability of the ground state of thulium atom was calculated theoretically in a wide range of wavelengths; the value found for it (195 a.u. at the wavelength $\lambda = 814.5$ nm) agrees with the result of the above experiment. This proves sufficiently high reliability of calculations, in spite of the considerable difficulties related to the calculation of energy levels and oscillator strengths for rare earth atoms with partially filled inner shells [24–26]. The waist size w_0 determined using Eqn (8) amounted to 124±12 μm, which agrees with the calculated value $w_0 = 111.3\pm1.4$ μm within the error limits. The waist size obtained from the formulae for the frequencies of parametric resonances is overestimated because the temperature of atoms in the experiment is comparable with the trap depth, which leads to essential anharmonicity of the potential [27]. In spite of the high uncertainty of the method, the agreement between the calculated and experimental values of the waist size means that the experimental estimate of the ground state polarisability is most likely valid.

4. Conclusions

We presented the results of studying ultracold thulium atoms trapped in an optical lattice formed in the external enhancement cavity at the wavelength 814.5 nm. The power enhancement coefficient of the cavity amounted to 8.5, which allowed one to achieve a power up to 25 W in the antinodes of the lattice and an efficiency of 60% for loading the atoms from the MOT to the optical lattice. The trapping potential of the optical lattice was characterised by analysing the parametric resonances. From the frequencies of the parametric resonances, we determined the polarisability of the ground state of thulium atom at the wavelength 814.5 nm that amounted to 146±44 a.u.

The enhancement cavity allowed a significant increase in the depth of the optical lattice potential, which in the future will be used in the experimental search for the magic wavelength of the clock transition at 1.14 μm in the thulium atom. Moreover, we plan to measure the differential scalar and tensor polarisability, as well as the differential static polarisability that determines the sensitivity of the clock transition frequency to the environmental thermal radiation.

Acknowledgements. The work was supported by the Russian Foundation for Basic Research (Grant Nos 18-02-00628 and 16-29-11723).

References

1. Hinkley N., Sherman J.A., Phillips N.B., Schioppo M., Lemke N.D., Beloy K., Pizzocaro M., Oates C.W., Ludlow A.D. *Science*, **341**, 1215 (2013).
2. Bloom B.J., Nicholson T.L., Williams J.R., Campbell S.L., Bishof M., Zhang X., Zhang W., Bromley S.L., Ye J. *Nature*, **506**, 71 (2014).
3. Chou C.W., Hume D.B., Rosenband T., Wineland D.J. *Science*, **329**, 1630 (2010).
4. Blatt S., Ludlow A.D., Campbell G.K., Thomsen J.W., Zelevinsky T., Boyd M.M., Ye J., Baillard X., Fouché M., Targat L.R., Brusch A., Lemonde P., Takamoto M., Hong F.-L., Kator H., Flambaum V.V. *Phys. Rev. Lett.*, **100**, 140801 (2008).
5. Müller J., Dirkx D., Kopeikin S.M., Lion G., Panet I., Petit G., Visser P.N.A.M. *Space Sci. Rev.*, **214**, 5 (2018).
6. Nicholson T.L., Campbell S.L., Hutson R.B., Marti G.E., Bloom B.J., McNally R.L., Zhang W., Barrett M.D., Safronova M.S., Strouse G.F., Tew W.L., Ye J. *Nat. Commun.*, **6**, 6896 (2015).
7. Schioppo M., Brown R.C., McGrew W.F., Hinkley N., Fasano R.J., Beloy K., Yoon T.H., Milani G., Nicolodi D., Sherman J.A., Phillips N.B., Oates C.W., Ludlow A.D. *Nat. Photonics*, **11**, 48 (2017).
8. Chen J.-S., Brewer S.M., Chou C.W., Wineland D.J., Leibrandt D.R., Hume D.B. *Phys. Rev. Lett.*, **118**, 053002 (2017).
9. Huntemann N., Sanner C., Lipphardt B., Tamm Chr., Peik E. *Phys. Rev. Lett.*, **116**, 063001 (2017).
10. Campbell C.J., Radnaev A.G., Kuzmich A., Dzuba V.A., Flambaum V.V., Derevianko A. *Phys. Rev. Lett.*, **108**, 120802 (2012).
11. Arnold K.J., Kaewuam R., Roy A., Tan T.R., Barrett M.D. arXiv:1712.00240 (2017).
12. Sukachev D., Fedorov S., Tolstikhina I., Tregubov D., Kalganova E., Vishnyakova G., Golovizin A., Kolachevsky N., Khabarova K., Sorokin V. *Phys. Rev. A*, **94**, 022512 (2016).
13. Katori H., Takamoto M., Pal'chikov V.G., Ovsiannikov V.D. *Phys. Rev. Lett.*, **91**, 173005 (2003).
14. Arora B., Safronova M.S., Clark C.W. *Phys. Rev. A*, **76**, 052509 (2007).
15. Takamoto M., Hong F., Higashi R., Katori H. *Nature*, **435**, 321 (2005).
16. Yi L., Mejri S., McFerran J.J., Coq Y.L., Bize S. *Phys. Rev. Lett.*, **106**, 073005 (2011).
17. Ovsiannikov V.D., Marmo S.I., Palchikov V.G., Katori H. *Phys. Rev. A*, **93**, 043420 (2016).
18. Brown R.C., Phillips N.B., Beloy K., McGrew W.F., Schioppo M., Fasano R.J., Milani G., Zhang X., Hinkley N., Leopardi H., Yoon T.H., Nicolodi D., Fortier T.M., Ludlow A.D. *Phys. Rev. Lett.*, **119**, 253001 (2017).
19. Lemonde P., Wolf P. *Phys. Rev. A*, **72**, 033409 (2005).
20. Sukachev D., Sokolov A., Chebakov K., Akimov A., Kanorsky S., Kolachevsky N., Sorokin V. *Phys. Rev. A*, **82**, 011405(R) (2010).
21. Sukachev D.D., Kalganova E.S., Sokolov A.V., Fedorov S.A, Vishnyakova G.A., Akimov A.V., Kolachevsky N.N., Sorokin V.N. *Quantum Electron.*, **44** (6), 515 (2014) [*Kvantovaya Elektron.*, **44** (6), 515 (2014)].
22. Hansch T., Couillaud B. *Opt. Commun.*, **35** (3), 441 (1980).
23. Friebel S., D'Andrea C., Walz J., Weitz M., Hansch T.W. *Phys. Rev. A*, **57**, R20 (1998).
24. Mitroy J., Safronova M.S., Clark C.W. *J. Phys. B: At. Mol. Opt. Phys.*, **43**, 202001 (2010).
25. Dzuba V.A., Kozlov A., Flambaum V.V. *Phys. Rev. A*, **89**, 042507 (2014).
26. Chu X., Dalgarno A., Groenenboom G.C. *Phys. Rev. A*, **75**, 032723 (2007).
27. Ravensbergen C., Corre V., Soave E., Kreyer M., Tzanova S., Kirilov E., Grimm R. arXiv:1801.05658 (2018).